

Scientific paper

Syntheses, Characterization, Crystal Structures and Antimicrobial Activity of Copper(II), Nickel(II) and Zinc(II) Complexes Derived from 5-Bromo-2-((cychlopentylimino)methyl)phenol

Li Zhang, Xiao-Yang Qiu* and Shu-Juan Liu

College of Science & Technology, Ningbo University, Ningbo 315315, P. R. China

* Corresponding author: E-mail: xiaoyang_qiu@126.com

Received: 08-12-2022

Abstract

Four new complexes of copper(II), nickel(II) and zinc(II), $[CuL_2]$ (1), $[Ni_3L_2(4-BrSal)_2(CH_3COO)_2(CH_3OH)_2]$ -2CH₃OH (2), $[ZnBr_2(HL)_2]$ (3) and $[ZnL(dca)]_n$ (4), where L is 5-bromo-2-((cychlopentylimino)methyl)phenolate, HL is the zwitterionic form of 5-bromo-2-((cychlopentylimino)methyl)phenol, 4-BrSal is the monoanionic form of 4-bromo-salicylaldehyde, dca is dicyanamide anion, were synthesized and characterized by elemental analysis, IR and UV-Vis spectroscopy. The structures of the complexes were further confirmed by single crystal X-ray structure determination. Complex 1 is a mononuclear copper(II) compound, with a crystallographic two-fold rotation axis symmetry. The Cu atom is in distorted square planar coordination. Complex 2 is a trinuclear nickel(II) compound, with an inversion center symmetry. The Ni atoms are in octahedral coordination. Complex 3 is a mononuclear zinc(II) compound, while complex 4 is a dca bridged polymeric zinc(II) compound. The Zn atoms are in tetrahedral coordination. The compounds were assayed for their antimicrobial activities.

Keywords: Schiff base, copper complex, nickel complex, zinc complex, antimicrobial activity

1. Introduction

The synthesis of new metal complexes with biological activities is a hot topic in coordination chemistry and bioinorganic chemistry. Among the complexes, those with Schiff base ligands have received particular attention due to their facile preparation, interesting structural diversity, and the possibility of the presence of various electron-donating or electron-withdrawing substituents. Schiff base copper, nickel and zinc complexes have been extensively studied and are considered as excellent alternatives for classic organic antibacterial, antifungal and antitumor.² Despite the presence of a large number of studies on the antibacterial activities of such complexes, it is still necessary to explore new complexes with more effective activities. It has been proved that the compounds with electron-withdrawing substituent groups can improve their antimicrobial ability.³ Rai et al. reported some compounds with fluoro, chloro, bromo, and iodo-substituted groups, and their remarkable antimicrobial property.⁴ Schiff base complexes of copper, nickel and zinc have potential antibacterial activities.⁵ Recently, our research group has reported some Schiff base complexes with biological properties.⁶ The platinum complexes with cyclopentylamine exhibited considerable cytotoxicity against cancer cell lines.⁷ Moreover, the complexes with cyclopentylamine Schiff base ligands have interesting antibacterial activity.⁸ In pursuit of new Schiff base complexes with potential antimicrobial activity, four new complexes [CuL₂] (1), [Ni₃L₂(4-BrSal)₂(CH₃COO)₂(CH₃OH)₂]·2CH₃OH (2), [ZnBr₂(HL)₂] (3) and [ZnL(dca)]_n (4), where L is 5-bromo-2-((cychlopentylimino)methyl)phenolate, HL is the zwitterionic form of 5-bromo-2-((cychlopentylimino)methyl)phenol, 4-BrSal is the monoanionic form of 4-bromosalicylaldehyde, dca is dicyanamide anion, and their antimicrobial activities are present.

2. Experimental

2. 1. Materials and Methods

4-Bromosalicylaldehyde, cyclopentylamine, copper acetate, nickel acetate, zinc bromide, zinc nitrate and sodi-

um dicyanamide were obtained from Sigma-Aldrich. All other chemicals were commercial obtained from Xiya Chemical Co. Ltd. Elemental analyses of C, H and N were carried out in a Perkin-Elmer automated model 2400 Series II CHNS/O analyzer. FT-IR spectra were obtained on a Perkin-Elmer 377 FT-IR spectrometer with samples prepared as KBr pellets. UV-Vis spectra were obtained on a Lambda 35 spectrometer. Single crystal structural X-ray diffraction was carried out on a Bruker APEX II CCD diffractometer. ¹H NMR data were recorded on a Bruker 500 MHz instrument. Molar conductivities of the complexes in DMSO solutions (10⁻³ M) at room temperature were measured using a Systronic model 303 direct reading conductivity meter.

2. 2. Synthesis of 2-bromo-6-((2-(isopropylamino)ethylimino)methyl) phenol (HL)

4-Bromosalicylaldehyde (1.0 mmol, 0.20 g) and cyclopentylamine (1.0 mmol, 0.085 g) were mixed and stirred in methanol (30 mL). The mixture was refluxed for 30 min, and with the solvent removed by distillation. The solid product was re-crystallized from methanol to give yellow product. Yield 93%. Anal. calc. for $C_{12}H_{14}BrNO$: C, 53.75; H, 5.26; N, 5.22; found: C, 53.62; H, 5.35; N, 5.31%. Characteristic IR data (cm⁻¹): 1637 (C=N). UV-Vis data (MeOH, λ_{max} , nm): 233, 272, 335. ¹H NMR (d_6 -DMSO, δ , ppm): 12.11 (s, 1H, OH), 8.63 (s, 1H, CH=N), 7.51 (d, 1H, ArH), 7.45 (s, 1H, ArH), 6.92 (d, 1H, ArH), 3.27 (m, 1H, CH), 1.89 (m, 2H, CH₂), 1.73 (m, 2H, CH₂), 1.50 (m, 2H, CH₂), 1.43 (m, 2H, CH₂).

2. 3. Synthesis of $[CuL_2]$ (1)

HL (0.10 mmol, 27 mg) and copper acetate monohydrate (0.10 mmol, 20 mg) mixed in methanol (15 mL) were stirred at room temperature for 30 min to give a clear blue solution. Block blue single crystals suitable for X-ray diffraction were grown from the solution upon slowly evaporation within 5 days. The crystals were isolated by filtration. Yield 41%. Anal. calc. for $C_{24}H_{26}Br_2CuN_2O_2$: C, 48.22; H, 4.38; N, 4.69; found: C, 48.03; H, 4.47; N, 4.57%. Characteristic IR data (cm⁻¹): 1621 ($\nu_{C=N}$). UV-Vis data (MeOH, λ_{max} , nm): 227, 248, 274, 361. Molar conductance (10⁻³ M in DMSO): 22 Ω^{-1} cm² mol⁻¹.

2. 4. Synthesis of [Ni₃L₂(4-BrSal)₂(CH₃COO)₂ (CH₃OH)₂]·2CH₃OH (2)

HL (0.10 mmol, 27 mg), 4-bromosalicylaldehyde (0.10 mmol, 20 mg) and nickel acetate tetrahydrate (0.10 mmol, 25 mg) mixed in methanol (15 mL) were stirred at room temperature for 30 min to give a clear green solution. Block green single crystals suitable for X-ray diffraction were grown from the solution upon slowly evaporation within 3

days. The crystals were isolated by filtration. Yield 53%. Anal. calc. for $C_{46}H_{56}Br_4N_2Ni_3O_{14}$: C, 40.73; H, 4.16; N, 2.06; found: C, 40.87; H, 4.05; N, 1.97%. Characteristic IR data (cm⁻¹): 1646 ($\nu_{C=O}$), 1632 ($\nu_{C=N}$), 1586 ($\nu_{as-acetate}$), 1405 ($\nu_{s-acetate}$). UV-Vis data (MeOH, λ_{max} , nm): 227, 245, 267, 362. Molar conductance (10⁻³ M in DMSO): 17 Ω^{-1} cm² mol⁻¹.

2. 5. Synthesis of $[ZnBr_2(HL)_2]$ (3)

HL (0.10 mmol, 27 mg) and zinc bromide (0.10 mmol, 23 mg) mixed in methanol (15 mL) were stirred at room temperature for 30 min to give a clear colorless solution. Block colorless single crystals suitable for X-ray diffraction were grown from the solution upon slowly evaporation within 8 days. The crystals were isolated by filtration. Yield 45%. Anal. calc. for C₂₄H₂₈Br₄N₂O₂Zn: C, 37.85; H, 3.71; N, 3.68; found: C, 37.71; H, 3.65; N, 3.77%. Characteristic IR data (cm⁻¹): 1628, 1633 ($\nu_{\rm C=N}$). UV-Vis data (MeOH, $\lambda_{\rm max}$, nm): 215, 260, 313, 370. Molar conductance (10⁻³ M in DMSO): 26 Ω^{-1} cm² mol⁻¹.

2. 6. Synthesis of $[ZnL(dca)]_n$ (4)

HL (0.10 mmol, 27 mg), sodium dicyanamide (0.10 mmol, 8.9 mg) and zinc nitrate hexahydrate (0.10 mmol, 30 mg) mixed in methanol (15 mL) were stirred at room temperature for 30 min to give a clear colorless solution. Block colorless single crystals suitable for X-ray diffraction were grown from the solution upon slowly evaporation within 4 days. The crystals were isolated by filtration. Yield 52%. Anal. calc. for C₁₄H₁₃BrN₄OZn: C, 42.19; H, 3.29; N, 14.06; found: C, 42.37; H, 3.40; N, 13.93%. Characteristic IR data (cm⁻¹): 2371, 2281, 2195 ($\nu_{\rm dca}$), 1618 ($\nu_{\rm C=N}$). UV-Vis data (MeOH, $\lambda_{\rm max}$, nm): 221, 245, 279, 360. Molar conductance (10⁻³ M in DMSO): 33 Ω^{-1} cm² mol⁻¹.

2. 7. X-ray Crystallography

X-ray diffraction was carried out at a Bruker APEX II CCD area diffractometer equipped with MoKα radiation ($\lambda = 0.71073 \text{ Å}$). The collected data were reduced with SAINT,9 and multi-scan absorption correction was performed using SADABS.¹⁰ The structures of the complexes were solved by direct method, and refined against F^2 by full-matrix least-squares method using SHELXTL.11 All of the non-hydrogen atoms were refined anisotropically. The H6 atom in complex 2, and H1 and H2 atoms in complex 3 were located from difference Fourier maps and refined isotropically, with O-H and N-H distances restrained to 0.85(1) and 0.90(1) Å, respectively. The remaining hydrogen atoms were placed in calculated positions and constrained to ride on their parent atoms. The cyclopentyl group in complex 2 is disordered over two sites, with occupancies of 0.45(3) and 0.55(3), respectively. The crystallographic data and refinement parameters for the complexes are listed in Table 1.

Table 1. Crystallographic and refinement data for the complexes

Complex	1	2	3	4
Formula	C ₂₄ H ₂₆ Br ₂ CuN ₂ O ₂	C ₄₆ H ₅₆ Br ₄ N ₂ Ni ₃ O ₁₄	$C_{24}H_{28}Br_4N_2O_2Zn$	C ₁₄ H ₁₃ BrN ₄ OZn
Formula weight	597.83	1356.69	761.49	398.56
Crystal system	Triclinic	Monoclinic	Monoclinic	Orthorhombic
Space group	P-1	$P2_1/c$	$P2_1/n$	Стса
a (Å)	9.4221(12)	11.2785(12)	17.6493(13)	7.4850(11)
b (Å)	10.0407(12)	12.2231(13)	8.8618(14)	19.0531(10)
c (Å)	12.6190(13)	20.7738(16)	18.0178(13)	22.4816(13)
α (°)	91.7950(10)	90	90	90
β (°)	91.5060(10)	93.9970(10)	99.451(2)	90
γ (°)	102.3690(10)	90	90	90
$V(Å^3)$	1164.9(2)	2856.9(5)	2779.8(5)	3206.2(5)
Z	2	2	4	8
$D_{\rm calc}$ (g cm ⁻³)	1.704	1.577	1.820	1.651
μ (Mo Ka) (mm ⁻¹)	4.391	3.834	6.656	4.027
F(000)	598	1364	1488	1584
Measured reflections	6293	14712	14377	8412
Unique reflections	4306	5317	5167	1619
Observed reflections $(I \ge 2\sigma(I))$	3140	2039	2902	1119
Parameters	280	365	304	115
Restraints	0	94	2	0
GOOF	1.006	0.972	1.012	1.027
R_1 , $wR_2 [I \ge 2\sigma(I)]^a$	0.0385, 0.0878	0.0825, 0.2402	0.0473, 0.1001	0.0409, 0.0982
R_1 , wR_2 (all data) ^a	0.0603, 0.0962	0.1966, 0.3189	0.1039, 0.1230	0.0709, 0.1118

^a $R_1 = \Sigma ||F_0| - |F_c||/\Sigma |F_0|$, $wR_2 = \{\Sigma [w(F_0^2 - F_c^2)^2]/\Sigma [w(F_0^2)^2]\}^{1/2}$

2. 8. Antimicrobial Assay

The antibacterial activity of the complexes was tested against Bacillus subtilis, Staphylococcus aureus, Escherichia coli, and Pseudomonas fluorescence using MH (Mueller-Hinton) medium. The antifungal activities of the compounds were tested against Candida albicans and Aspergillus niger using RPMI-1640 medium. The MIC values of the tested compounds were determined by a colorimetric method using the dye MTT.¹² A stock solution of the compound (150 µg mL⁻¹) in DMSO was prepared and graded quantities (75 μ g mL⁻¹, 37.5 μ g mL⁻¹, 18.8 μ g mL⁻¹, 9.4 μ g mL^{-1} , 4.7 μ g mL^{-1} , 2.3 μ g mL^{-1} , 1.2 μ g mL^{-1} , 0.59 μ g mL^{-1}) were incorporated in specified quantity of the corresponding sterilized liquid medium. A specified quantity of the medium containing the compound was poured into micro-titration plates. Suspension of the microorganism was prepared to contain approximately 1.0×10^5 cfu mL⁻¹ and applied to microtitration plates with serially diluted compounds in DMSO to be tested and incubated at 37 °C for 24 h and 48 h for bacteria and fungi, respectively. Then the MIC values were visually determined on each of the microtitration plates, 50 µL of PBS (phosphate buffered saline $0.01 \text{ mol } L^{-1}$, pH = 7.4) containing 2 mg of MTT mL⁻¹ was added to each well. Incubation was continued at room temperature for 4-5 h. The content of each well was removed and 100 μ L solution of isopropanol (95%) and 1 mol L-1 HCl (5%) was added to extract the dye. After 12 h of incubation at room temperature, the optical density was measured with a microplate reader at 550 nm.

3. Results and Discussion

3. 1. Synthesis and Characterization

The Schiff base HL was readily prepared by the reaction of equimolar quantities of 4-bromosalicylaldehyde and cyclopentylamine in methanol. The complexes 1-4 were prepared by the reaction of HL with copper acetate, nickel acetate, zinc bromide, and zinc nitrate and sodium dicyanamide, respectively in methanol (Scheme 1). Single crystals of the complexes were obtained by slow evaporation of their methanolic solution. Elemental analyses of the complexes are in accordance with the molecular structures determined by the single crystal X-ray analysis.

Scheme 1. The synthetic procedure for HL and the complexes.

3. 2. Spectroscopic Studies

The typical and strong absorptions at 1637 cm⁻¹ for HL and 1618-1632 cm⁻¹ for the complexes are generated by the vibrations of the C=N bonds, indicating the formation of the Schiff bases from the condensation reaction of the 4-bromosalicylaldehyde and cyclopentylamine during the coordination.¹³ The strong band at 1646 cm⁻¹ for com-

plex **2** can be assigned to the C=O absorption of the 4-bromosalicylaldehyde ligand. Complex **2** exhibit two bands at 1586 cm⁻¹ for $\nu_{\text{as-acetate}}$ and 1405 cm⁻¹ for $\nu_{\text{s-acetate}}$.¹⁴ The separation between the two bands is 181 cm⁻¹, which can be correlated to the bidentate acetate groups.¹⁴ The characteristic bands at 2371, 2281 and 2195 cm⁻¹ in the spectrum of complex **4** can be assigned to the vibrations of the dicyanamide ligands.¹⁵

In the UV-Vis spectra of HL and the complexes, the bands at 360-370 nm are attributed to the azomethine chromophore $\pi \rightarrow \pi^*$ transition. The bands at higher energies (210-230 and 245-280 nm) are associated with the benzene $\pi \rightarrow \pi^*$ transition. The bands at higher energies (210-230 and 245-280 nm) are associated with the benzene $\pi \rightarrow \pi^*$ transition.

3. 3. Structure Description of Complex 1

Selected bond lengths and angles for complex 1 are listed in Table 2. Molecular structure of the complex is shown in Figure 1. The Cu atom is coordinated in square planar geometry, with two phenolate O and two imino N

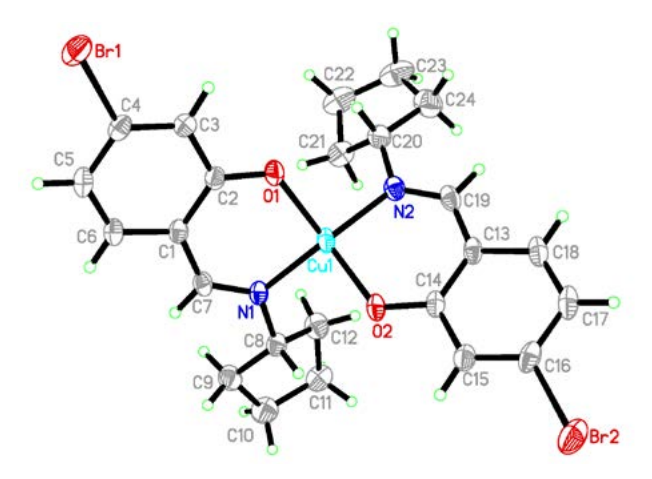


Figure 1. A perspective view of complex **1** with the atom labeling scheme. Thermal ellipsoids are drawn at the 30% probability level.

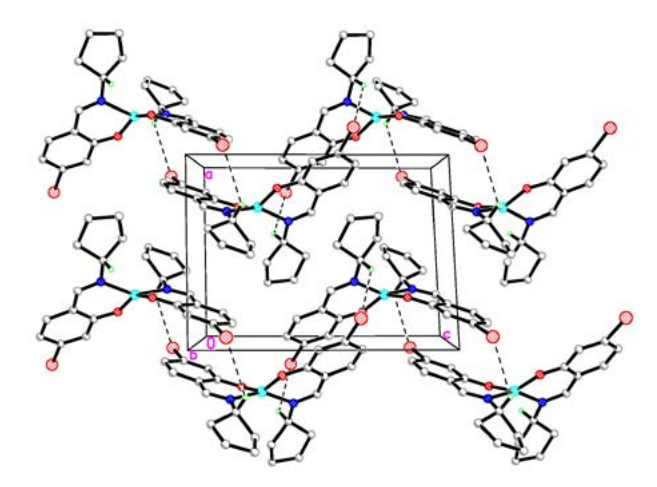


Figure 2. The crystal structure of complex 1, viewed along the b axis. Hydrogen bonds are shown as dashed lines.

atoms from two Schiff base ligands. The Schiff base ligands, act as bidentate ligands, chelate the Cu atom by generating two six-membered rings with bite angles of 94.20(11)° and 94.61(12)°. The *trans* angles are 147.92(12)° and 151.50(12)°, indicating the coordination is tetrahedrally distorted. The dihedral angle between the O1-Cu1-N1 and O2-Cu1-N2 planes is 41.8(2)°. The coordinate bond lengths and angles are comparable to those in the reported Schiff base copper complexes.¹⁷ The dihedral angle between the two benzene rings of the two Schiff base ligands is 35.7(3)°.

In the crystal structure of the complex, molecules are linked through intermolecular C-H···Br hydrogen bonds (Table 3), to form chains running along the *c* axis (Figure 2).

3. 4. Structure Description of Complex 2

Selected bond lengths and angles for complex 2 are listed in Table 2. Molecular structure of the complex is shown in Figure 3. The compound contains a centrosymmetric trinuclear nickel complex molecule and two methanol molecules of crystallization. The inversion center is located at the site of Ni2 atom. There are three bridges across the Ni···Ni atom pairs, involving two phenolate O atoms from a Schiff base ligand and a 4-bromosalicylaldehyde ligand, and an O–C–O moiety of a μ_2 - η^1 : η^1 -OAc group. The acetate bridges linking the central and terminal nickel atoms are mutually *trans*. The trinuclear nickel complex molecule consists of two NiL units connected to each other by a completely encapsulated third metal atom, Ni2. The adjacent Ni1···Ni2 distance is 3.070(1) Å.

The cage of Ni2 is formed by phenolate bridges, O1 and O2, from the Schiff base and 4-bromosalicylaldehyde ligands, and by two O atoms from two μ_2 - η^1 : η^1 -OAc ligands that furthermore connect the central metal with the two outer metal atoms resulting in an octahedral environment. The coordination around Ni2 atom displays only slight distortion. The bond distances Ni–O are relatively similar and range from 2.063(7) to 2.089(7) Å. The greatest deviation of the bond angles from those expected for an ideal octahedral geometry is found for O1–Ni2–O2 with 76.6(3)°, and O1–Ni2–O2A with 103.4(3)°. The remaining bond angles are close to the ideal values for the octahedral coordination.

The coordination around the inversion-related terminal Ni atoms, Ni1 and Ni1A, is also octahedral, with one imino N and one phenolate O atoms of a Schiff base ligand, and one carbonyl O and one phenolate O atoms of a 4-bromosalicylaldehyde ligand, defining the equatorial plane, and with two O atoms respectively from a methanol and a μ_2 - η^1 - η^1 -OAc ligand occupying the axial positions. The coordination around the terminal metal atoms also displays slight distortion. The greatest deviation of the bond angles from those expected for an ideal octahedral geometry is O1–Ni1–O2 (79.9(3)°), which is caused by the strain created by the four-membered chelate ring Ni1–O1–Ni2–O2.

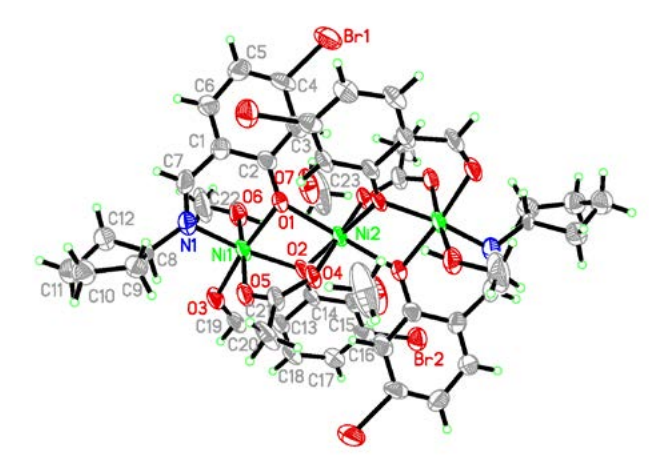


Figure 3. A perspective view of complex **2** with the atom labeling scheme. Thermal ellipsoids are drawn at the 30% probability level. The unlabeled atoms are related to the symmetry operation 1 - x, 1 - y, 1 - z.

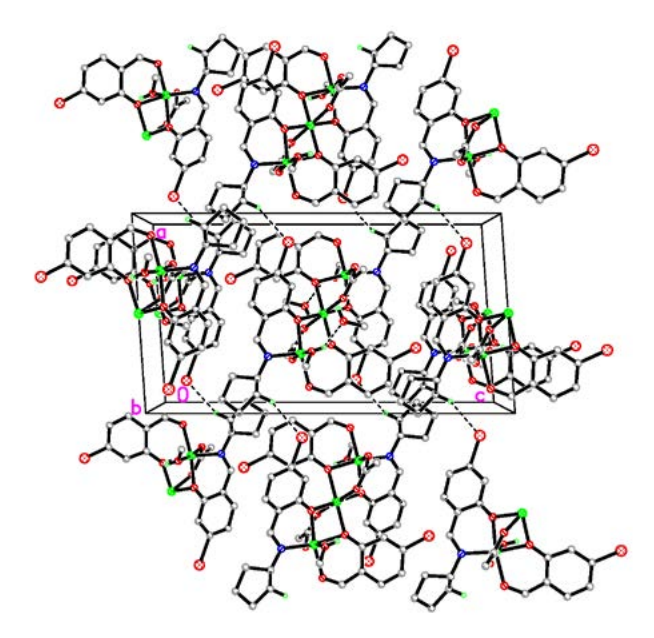


Figure 4. The crystal structure of complex 2, viewed along the b axis. Hydrogen bonds are shown as dashed lines.

The coordinate bond lengths and angles are comparable to those in the reported Schiff base nickel complexes. ¹⁸ The NiL units in the complex are butterfly-shaped, with the dihedral angle formed by the two benzene rings of the Schiff base ligand and 4-bromosalicylaldehyde ligand of 34.5(4)°.

In the crystal structure of the complex, molecules are linked through intermolecular C-H···Br hydrogen bonds (Table 3), to form chains running along the *a* axis (Figure 4).

3. 5. Structure Description of Complex 3

Selected bond lengths and angles for complex 3 are listed in Table 2. Molecular structure of the complex is

shown in Figure 5. The Zn atom is coordinated in tetrahedral geometry, with two phenolate O atoms from two zwitterionic Schiff base ligands. The coordinate bond angles are 102.33(12)–119.46(4)°, indicating it is deviated from ideal tetrahedral geometry. The coordinate bond lengths and angles are comparable to those in the reported Schiff base zinc complexes. ¹⁹ The dihedral angle between the two benzene rings of the two Schiff base ligands is 59.4(5)°.

In the crystal structure of the complex, molecules are linked through intermolecular C-H···Br hydrogen bonds (Table 3), to form chains running along the *b* axis (Figure 6).

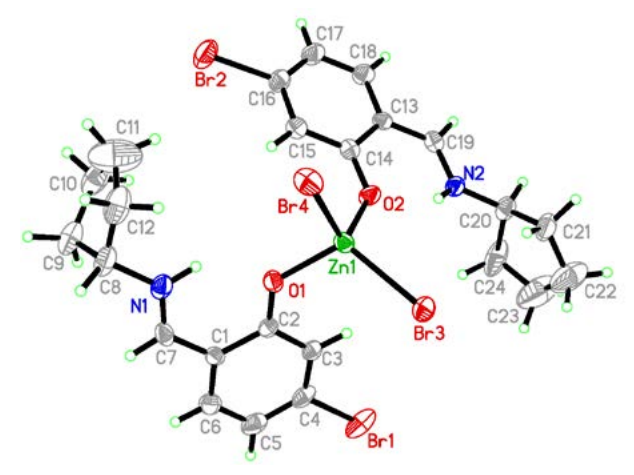


Figure 5. A perspective view of complex **3** with the atom labeling scheme. Thermal ellipsoids are drawn at the 30% probability level.

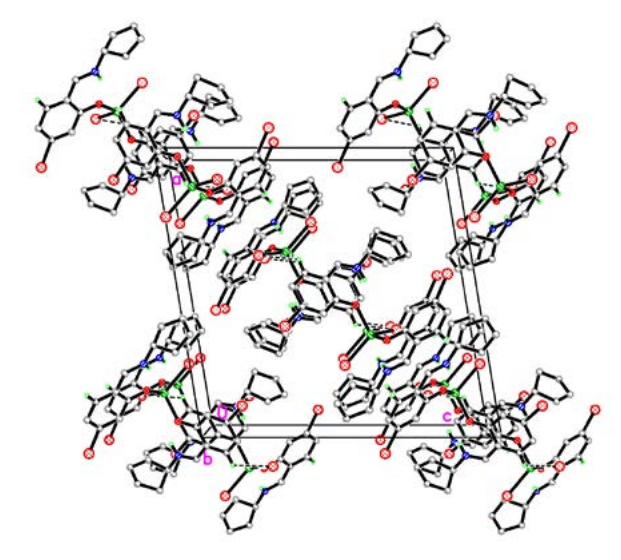


Figure 6. The crystal structure of complex $\bf 3$, viewed along the b axis. Hydrogen bonds are shown as dashed lines.

3. 6. Structure Description of Complex 4

Selected bond lengths and angles for complex 4 are listed in Table 2. Molecular structure of the complex is

shown in Figure 7. The compound is a dicyanamide bridged polymeric zinc complex. Each Zn atom is coordinated in tetrahedral geometry, with one phenolate O and one imino N atoms of the Schiff base ligand, and two N atoms of dicyanamide ligand. The coordinate bond angles are 99.12(18)–115.32(13)°, indicating it is deviated from ideal tetrahedral geometry. The coordinate bond lengths and angles are comparable to those in the reported Schiff base zinc complexes with dicyanamide bridges.²⁰

In the crystal structure of the complex, the [ZnL] units are linked through dicyanamide ligands, to form an infinite one-dimensional chain along the *a* axis. The chains are further linked through intermolecular C-H···N hydrogen bonds (Table 3) at the axis-*b* direction, to form two dimensional sheet parallel to the *ab* plane (Figure 6).

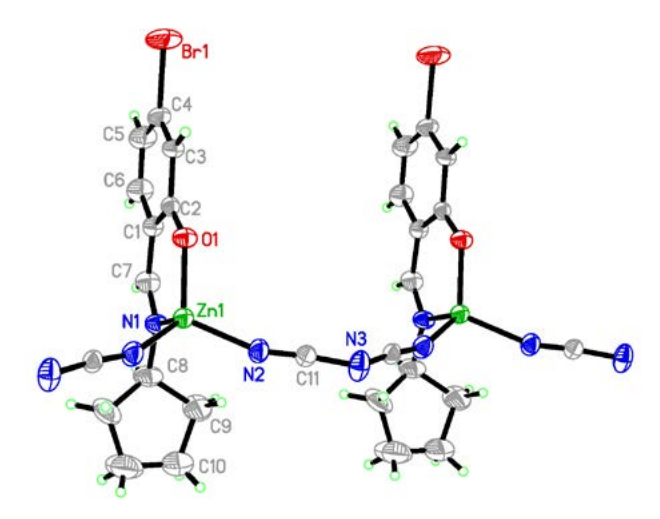


Figure 7. A perspective view of complex **4** with the atom labeling scheme. Thermal ellipsoids are drawn at the 30 % probability level. The unlabeled atoms are related to the symmetry operation 1 - x, y, z.

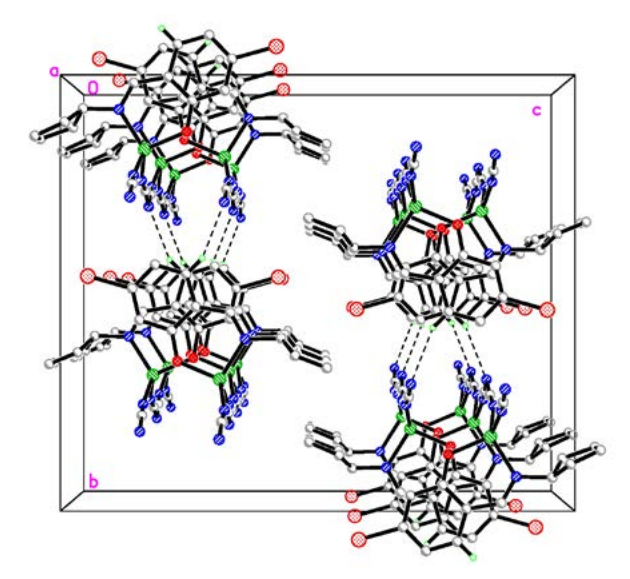


Figure 8. The crystal structure of complex 4, viewed along the a axis. Hydrogen bonds are shown as dashed lines.

Table 2. Selected bond distances (Å) and angles (°) for the complexes

1			
Cu1-O1	1.886(3)	Cu1-O2	1.883(3)
Cu1-N1	1.961(3)	Cu1-N2	1.950(3)
O2-Cu1-O1	147.92(12)	O2-Cu1-N2	94.61(12)
O1-Cu1-N2	93.42(12)	O2-Cu1-N1	93.36(11)
O1-Cu1-N1	94.20(11)	N2-Cu1-N1	151.50(12)
2			
Ni1-O1	2.002(7)	Ni1-O2	2.006(7)
Ni1-O3	2.026(8)	Ni1-N1	2.003(10)
Ni1-O5	2.039(8)	Ni1-O6	2.103(8)
Ni2-O1	2.063(7)	Ni2-O4	2.075(7)
Ni2-O4	2.075(7)	Ni2-O2	2.089(7)
N1-Ni1-O1	91.0(4)	N1-Ni1-O2	170.7(4)
O1-Ni1-O2	79.9(3)	N1-Ni1-O3	97.7(4)
O1-Ni1-O3	170.7(3)	O2-Ni1-O3	91.5(3)
N1-Ni1-O5	90.1(4)	O1-Ni1-O5	97.4(3)
O2-Ni1-O5	88.8(3)	O3-Ni1-O5	86.0(3)
N1-Ni1-O6	91.5(4)	O1-Ni1-O6	90.2(3)
O2-Ni1-O6	90.8(3)	O3-Ni1-O6	86.2(3)
O5-Ni1-O6	172.2(4)	O1-Ni2-O1A	180
O1-Ni2-O4A	91.8(3)	O1-Ni2-O4	88.2(3)
O1-Ni2-O4A	91.8(3)	O4-Ni2-O4A	180
O1-Ni2-O2A	103.4(3)	O4-Ni2-O2A	89.2(3)
O1-Ni2-O2	76.6(3)	O1-Ni2-O2A	103.4(3)
O4-Ni2-O2A	89.2(3)	O4-Ni2-O2	90.8(3)
O2-Ni2-O2A	180		

Symmetry code for A: 1 - x, 1 - y, 1 - z.

3			
Zn1-Br3	2.3629(10)	Zn1-Br4	2.3546(10)
Zn1-O1	1.954(4)	Zn1-O2	1.942(4)
O2-Zn1-O1	107.36(18)	O2-Zn1-Br4	111.25(12)
O1-Zn1-Br4	102.33(12)	O2-Zn1-Br3	103.42(12)
O1-Zn1-Br3	112.70(13)	Br4-Zn1-Br3	119.46(4)
4			
Zn1-O1	1.907(4)	Zn1-N2	1.966(4)
Zn1-N1	1.980(5)		
O1-Zn1-N2	111.45(12)	O1-Zn1-N2A	111.45(12)
N2-Zn1-N2A	104.4(2)	O1-Zn1-N1	99.12(18)
N2-Zn1-N1	115.32(13)		

Symmetry code for A: 1 – x, y, z.

3. 4. Antimicrobial Activity

The complexes as well as HL and related inorganic metal salts were screened for antibacterial activities against two Gram (+) bacterial strains (*Bacillus subtilis* and *Staphylococcus aureus*) and two Gram (-) bacterial strains (*Escherichia coli* and *Pseudomonas fluorescence*) by MTT method. The MIC (minimum inhibitory concentration, μ g mL⁻¹) values of the compounds against four bacteria are listed in Table 4. Penicillin G was used as the standard drug. As a result, the complexes have better activities

D-H···A	d(D-H)	d(HA)	$d(D\cdots A)$	Angle (D-H···A)
1 C8-H8···Br1 ^{#1} 2	0.98	3.04(3)	3.723(5)	128(6)
C12-H12D···Br1 ^{#2}	0.97	2.79(4)	3.694(6)	155(7)
C6-H6···Br4 ^{#3}	0.93	3.05(4)	3.671(7)	125(6)
C6-H6···N3 ^{#4}	0.93	2.51(3)	3.379(1)	156(3)

Table 3. Hydrogen bond distances (Å) and angles (°) for the complexes

Symmetry codes: #1: 2 - x, 1 - y, - z; #2: 1 + x, y, z; #3: 1 - x, 2 - y, 1 - z; #4: 1/2 + x, -1/2+ *y*, *z*.

against all the bacteria than the free Schiff base HL and the related inorganic metal salts. Complexes 1 and 3 show strong activity against B. subtilis, S. aureus and E. coli, while weak activity against P. fluorescence. Complex 2 shows medium activity against B. subtilis, and weak activity against S. aureus, E. coli and P. fluorescence. Complex 4 shows strong activity against B. subtilis and S. aureus, medium activity against E. coli, while weak activity against P. fluorescence. Complexes 1, 3 and 4 have stronger activity against all the bacteria than Penicillin G. Complex 2 has stronger activity against E. coli and P. fluorescence, while weaker activity against B. subtilis and S. aureus than Penicillin G. However, all the complexes have no activity on the fungal strains Candida albicans and Aspergillus niger.

Table 4. Antibacterial activities of the assayed compounds with minimum inhibitory concentrations (µg mL⁻¹)

Tested material	B. subtilis	S. aureus	E. coli	P. fluorescence
1	1.2	2.3	4.7	18.8
2	9.4	18.8	18.8	37.5
3	2.3	4.7	4.7	37.5
4	4.7	2.3	9.4	75
HL	18.8	37.5	37.5	> 150
Copper acetate	9.4	4.7	9.4	37.5
Nickel acetate	37.5	37.5	> 150	> 150
Zinc bromide	18.8	18.8	75	> 150
Zinc nitrate	18.8	18.8	75	> 150
Penicillin G	2.3	4.7	>150	> 150

4. Conclusion

Four new copper, nickel and zinc complexes derived from the Schiff base 5-bromo-2-((cychlopentylimino)methyl)phenol were synthesized and characterized by infrared and electronic spectra. The detailed structures of the complexes have been confirmed by single crystal X-ray structure determination. The complexes have strong activities against the bacteria B. subtilis, S. aureus and E. coli, which deserve further study.

Acknowlegments

This work was financially supported by Ningbo Public Welfare Funds (Project No. 2021S142), and College of Science & Technology Ningbo University (Project No. hx2022010).

Supplementary Data

CCDC 2192715 (1), 2192716 (2), 2192718 (3) and 2192719 (4) contain the supplementary crystallographic data for the compounds. These data can be obtained free of charge via http://www.ccdc.cam.ac.uk/conts/retrieving. html, or from the Cambridge Crystallographic Data Centre, 12 Union Road, Cambridge CB2 1EZ, UK; fax: (+44) 1223-336-033; or e-mail: deposit@ccdc.cam.ac.uk.

5. References

1. (a) A. Jurowska, W. Serafin, M. Hodorowicz, K. Kruczala, J. Szklarzewicz, Polyhedron 2022, 222, 115903;

DOI:10.1016/j.poly.2022.115903

(b) Y. Yuan, X. K. Lu, G. Q. Zhou, X.-Y. Qiu, Acta Chim. Slov. 2021, 68, 1008-1015; DOI:10.17344/acsi.2021.7070

(c) S. Han, Y. Wang, Acta Chim. Slov. 2021, 68, 961-969;

DOI:10.17344/acsi.2021.6965

(d) W.Y. Shen, C.P. Jia, L.Y. Liao, L.L. Chen, C. Hou, Y.H. Liu, H. Liang, Z.F. Chen, J. Med. Chem. 2022, 65, 5134-5148.

DOI:10.1021/acs.jmedchem.2c00133

2. (a) M.S. Ragab, M.H. Soliman, M.R. Shehata, M.M. Shoukry, M.A. Ragheb, Appl. Organomet. Chem. 2022, e6802;

(b) M. Bencela, S.S. Kumari, Polyhedron 2022, 219, 115788; DOI:10.1016/j.poly.2022.115788

(c) H. Goudarziafshar, S. Yousefi, Y.A. Tyula, M. Dusek, V. Eigner, RSC Advances 2022, 12, 13580-13592;

DOI:10.1039/D2RA00719C

(d) S. Esmaielzadeh, E. Zarenezhad, Acta Chim. Slov. 2018, 65, 416-428; DOI:10.17344/acsi.2018.4159

(e) D.L. Peng, N. Sun, Acta Chim. Slov. 2018, 65, 895-901; DOI:10.17344/acsi.2018.4543

(f) C.L. Zhang, X.Y. Qiu, S.J. Liu, Acta Chim. Slov. 2019, 66,

- 484-489; **DOI:**10.17344/acsi.2019.5019
- (g) S.F. Yu, X.Y. Qiu, S.J. Liu, Acta Chim. Slov. 2020, 67, 1301-1308; DOI:10.17344/acsi.2020.6321
- (h) A.S. Hossain, J.M. Mendez-Arriaga, C.K. Xia, J.M. Xie, S. Gomez-Ruiz, *Polyhedron* **2022**, *217*, 115692.

DOI:10.1016/j.poly.2022.115692

 (a) G. Paraskevopoulos, S. Monteiro, R. Vosatka, M. Kratky, L. Navratilova, F. Trejtnar, J. Stolarikova, J. Vinsova, *Bioorg. Med. Chem.* 2017, 25, 1524–1532;

DOI:10.1016/j.bmc.2017.02.053

(b) M. Zhang, D.-M. Xian, H.-H. Li, J.-C. Zhang, Z.-L. You, *Aust. J. Chem.* **2012**, *65*, 343–350;

DOI:10.1071/CH11424

- (c) H.-F. Guo, Y. Pan, D.-Y. Ma, P. Yan, Chinese J. Inorg. Chem. **2013**, 29, 1447–1453.
- 4. N. P. Rai, V. K. Narayanaswamy, T. Govender, B. K. Manuprasad, S. Shashikanth, P. N. Arunachalam, *Eur. J. Med. Chem.* **2010**, 45, 2677–2682.

DOI:10.1016/j.ejmech.2010.02.021

- (a) H. Kargar, M. Fallah-Mehrjardi, R. Behjatmanesh-Ardakani, H.A. Rudbari, A.A. Ardakani, S. Sedighi-Khavidak, K.S. Munawar, M. Ashfaq, M.N. Tahir, *Inorg. Chim. Acta* 2022, 530, 120677; DOI:10.1016/j.ica.2021.120677
 - (b) T. Vijayan, J. Kim, M. Azam, S.I. Al-Resayes, A. Stalin, B.S. Kannan, A. Jayamani, A. Ayyakannu, S. Nallathambi, *Appl. Organomet. Chem.* **2022**, *36*, e6542;

DOI:10.1002/aoc.6542

- (c) J.L. Hou, H.Y. Wu, C.B. Sun, Y. Bi, W. Chen, *Acta Chim. Slov.* **2020**, *67*, 860-865; **DOI**:10.17344/acsi.2020.5824
- (d) L.W. Xue, X. Fu, G.Q. Zhao, Q.B. Li, *Acta Chim. Slov.* **2021**, *68*, 17-24. **DOI**:10.17344/acsi.2020.5817
- (a) C.-L. Zhang, X.-Y. Qiu, S.-J. Liu, Acta Chim. Slov. 2019, 66, 719-725; DOI:10.17344/acsi.2019.5241
 - (b) L.-Y. He, X.-Y. Qiu, J.-Y. Cheng, S.-J. Liu, S.-M. Wu, *Polyhedron* **2018**, *156*, 105–110;

DOI:10.1016/j.poly.2018.09.017

(c) S. M. Wu, X. Y. Qiu, J. C. Wang, S. J. Liu, L. Y. He, Russ. J. Coord. Chem. 2019, 45, 378-384.

DOI:10.1134/S1070328419040109

- (a) C. Marzano, S. M. Sbovata, V. Gandin, D. Colavito, E. Del Giudice, R. A. Michelin, A. Venzo, R. Seraglia, F. Benetollo, M. Schiavon, R. Bertani, *J. Med. Chem.* 2010, 53, 6210–6227; DOI:10.1021/jm1006534
 - (b) J. Zhao, S. H. Gou, G. Xu, *Inorg. Chim. Acta* **2014**, 409, 310-314. **DOI:**10.1016/j.ica.2013.09.034
- X. Zhou, X.-F. Meng, W.-N. Li, C. Li, J.-J. Ma, Synth. React. Inorg. Met.-Org. Nano-Met. Chem. 2016, 46, 202-205.
 DOI:10.1080/15533174.2014.963241
- 9. Bruker, SMART (Version 5.625) and SAINT (Version 6.01). Bruker AXS Inc., Madison, Wisconsin, USA, 2007.
- G. M. Sheldrick, SADABS. Program for Empirical Absorption Correction of Area Detector, University of Göttingen, Germany, 1996.
- G. M. Sheldrick, SHELXTL V5.1 Software Reference Manual, Bruker AXS, Inc., Madison, Wisconsin, USA, 1997.
- 12. J. Meletiadis, J. F. G. M. Meis, J. W. Mouton, J. P. Donnelly, P.

- E. Verweij, *J. Clin. Microbiol.* **2000**, *38*, 2949–2954. **DOI**:10.1128/JCM.38.8.2949-2954.2000
- 13. (a) S. Manna, E. Zangrando, H. Puschmann, S.C. Manna, *Polyhedron* 2019, *162*, 285-292; DOI:10.1016/j.poly.2019.01.057
 (b) P. Chakraborty, S. Majumder, A. Jana, S. Mohanta, *Inorg. Chim. Acta* 2014, *410*, 65-75.
- 14. (a) B. Sarkar, M.G.B. Drew, M. Estrader, C. Diaz, A. Ghosh, *Polyhedron* **2008**, *27*, 2625–2633;

DOI:10.1016/j.poly.2008.05.004

DOI:10.1016/j.ica.2013.10.013

- (b) U. Kumar, J. Thomas, N. Thirupathi, *Inorg. Chem.* **2010**, 49, 62–72; **DOI**:10.1021/ic901100z
- (c) B.-H. Ye, X.-Y. Li, I.D. Williams, X.-M. Chen, *Inorg. Chem.* **2002**, *41*, 6426-6431. **DOI**:10.1021/ic025806+
- (a) P. Talukder, S. Shit, A. Sasmal, S.R. Batten, B. Moubaraki, K.S. Murray, S. Mitra, *Polyhedron* **2011**, *30*, 1767–1773;
 DOI:10.1016/j.poly.2011.03.049
 - (b) K. Bhar, S. Chattopadhyay, S. Khan, R.K. Kumar, T.K. Maji, J. Ribas, B.K. Ghosh, *Inorg. Chim. Acta* **2011**, *370*, 492-498; **DOI**:10.1016/j.ica.2011.02.055
 - (c) A. Ray, G. Pilet, C.J. Gomez-Garcia, S. Mitra, *Polyhedron* **2009**, *28*, 511–520. **DOI:**10.1016/j.poly.2008.11.054
- (a) M. F. Iskander, T. E. Khalil, R. Werner, W. Haase, I. Svoboda, H. Fuess, *Polyhedron* 2000, *19*, 949-958;
 DOI:10.1016/S0277-5387(00)00340-5
 - (b) S. Chandra, A. K. Sharma, *J. Coord. Chem.* **2009**, *62*, 3688-3700. **DOI**:10.1080/00958970903121305
- 17. (a) X.W. Dong, Y.G. Li, Z.W. Li, Y.M. Cui, H.L. Zhu, *J. Inorg. Biochem.* **2012**, *108*, 22-29;

DOI:10.1016/j.jinorgbio.2011.12.006

- (b) C. Senol, Z. Hayvali, H. Dal, T. Hokelek, *J. Mol. Struct.* **2011**, 997, 53-59. **DOI:**10.1016/j.molstruc.2011.04.037
- 18. (a) L.-W. Xue, Q.-L. Peng, P.-P. Wang, H.-J. Zhang, *Acta Chim. Slov.* **2019**, *66*, 694–700;

DOI:10.17344/acsi.2019.5151

- (b) H. Adams, D.E. Fenton, P.E. McHugh, *Inorg. Chem. Commun.* **2004**, *7*, 147–150. **DOI**:10.1016/j.inoche.2003.09.026
- R.-H. Hui, P. Zhou, Z.-L. You, Synth. React. Inorg. Met.-Org. Nano-Met. Chem. 2008, 38, 464–467.

DOI:10.1080/15533170802255476

Q. Shi, L. Sheng, K. Ma, Y. Sun, X. Cai, R. Liu, S. Wang, *Inorg. Chem. Commun.* 2009, 12, 255–258.

DOI:10.1016/j.inoche.2008.12.024

Povzetek

Sintetizirali smo štiri nove komplekse bakra(II), niklja(II) in cinka(II), $[CuL_2]$ (1), $[Ni_3L_2(4-BrSal)_2(CH_3COO)_2(CH_3OH)_2]\cdot 2CH_3OH$ (2), $[ZnBr_2(HL)_2]$ (3) in $[ZnL(dca)]_n$ (4), pri čemer je L = 5-bromo-2-((ciklopentilimino)metil)fenolat, HL je 5-bromo-2-((ciklopentilimino)metil)fenol v zwitterionski obliki, 4-BrSal je monoanionska oblika 4-bromosalicilaldehida, dca je dicianamidni anion. Produkte smo karakterizirali z elementno analizo, IR in UV-Vis spektroskopijo. Strukture kompleksov smo določili z monokristalno rentgensko difrakcijo. Kompleks 1 je enojedrna spojina bakra(II) z dvoštevno rotacijsko simetrijo in atomom Cu v popačeni kvadratno planarni koordinaciji. Kompleks 2 je trijedrna spojina niklja(II) s centrom inverzije in atomi Ni v oktaedrični koordinaciji. Kompleks 3 je enojedrna spojina cinka(II), kompleks 4 pa polimerna spojina cinka(II) z mostovnimi ligandi dca. Cinkovi atomi so v tetraedrični koordinaciji. Preiskovali smo antimikrobno aktivnost dobljenih produktov.



Except when otherwise noted, articles in this journal are published under the terms and conditions of the Creative Commons Attribution 4.0 International License